



Research Article

Open Access



Selective electroreduction of CO₂ to C₂₊ products on cobalt decorated copper catalysts

Sanaz Soodi^{1,2,3,4,#}, Jun-Jun Zhang^{5,6,#}, Jie Zhang^{1,2}, Yuefeng Liu⁷ , Mohsen Lashgari^{3,8}, Spyridon Zafeiratos⁹, Andreas Züttel^{1,2}, Kun Zhao^{1,2,10,*}, Wen Luo^{5,*} 

¹Laboratory of Materials for Renewable Energy (LMER), Institute of Chemical Sciences and Engineering (ISIC), Basic Science Faculty (SB), École Polytechnique Fédérale de Lausanne (EPFL) Valais/Wallis, Energypolis, Sion CH-1951, Switzerland.

²Empa Materials Science & Technology, Dübendorf CH-8600, Switzerland.

³Chemistry department, Institute for Advanced Studies in Basic Sciences (IASBS), Zanjan 45137-66731, Iran.

⁴Department of Chemical and Process Engineering, University of Surrey, Guildford GU2 7XH, UK.

⁵School of Environmental and Chemical Engineering, Shanghai University, Shanghai 200444, China.

⁶Department of Chemical Engineering, Sichuan University, Chengdu 610065, Sichuan, China.

⁷Dalian National Laboratory for Clean Energy (DNL), Dalian Institute of Chemical Physics (DICP), Chinese Academy of Science, Dalian 116023, Liaoning, China.

⁸Center for Research in Climate Change and Global Warming: Hydrogen and Solar Division, Zanjan 45137-66731, Iran.

⁹Institute for Chemistry and Energy, Environment and Health processes (ICPEES) - UMR 7515 CNRS - University of Strasbourg, Strasbourg 67087, France.

¹⁰Department of Chemistry, University of Washington, Seattle, WA 98195-1700, USA.

Authors contributed equally.

* **Correspondence to:** Dr. Kun Zhao, Laboratory of Materials for Renewable Energy (LMER), Institute of Chemical Sciences and Engineering (ISIC), Basic Science Faculty (SB), École Polytechnique Fédérale de Lausanne (EPFL) Valais/Wallis, Energypolis, Rue de l'Industrie 17, Sion CH-1951, Switzerland. Email: kzhao20@uw.edu; Prof. Wen Luo, School of Environmental and Chemical Engineering, Shanghai University, 99 Shangda Road, Shanghai 200444, China. E-mail: wenluo@shu.edu.cn

How to cite this article: Soodi S, Zhang JJ, Zhang J, Liu Y, Lashgari M, Zafeiratos S, Züttel A, Zhao K, Luo W. Selective electroreduction of CO₂ to C₂₊ products on cobalt decorated copper catalysts. *Chem Synth* 2024;4:44. <https://dx.doi.org/10.20517/cs.2024.11>

Received: 29 Jan 2024 **First Decision:** 6 May 2024 **Revised:** 20 May 2024 **Accepted:** 23 May 2024 **Published:** 6 Aug 2024

Academic Editor: Xiang-Dong Yao **Copy Editor:** Pei-Yun Wang **Production Editor:** Pei-Yun Wang

Abstract

Cu-catalyzed electrochemical CO₂ reduction reaction (CO₂RR) to multi-carbon (C₂₊) products is often plagued by low selectivity because the adsorption energies of different reaction intermediates are in a linear scaling relationship. Development of Cu-based bimetallic catalysts has been considered as an attractive strategy to address this issue; however, conventional bimetallic catalysts often avoid metals with strong CO adsorption energies to prevent surface poisoning. Herein, we demonstrated that limiting the amount of Co in CuCo bimetallic catalysts can enhance C₂₊ product selectivity. Specifically, we synthesized a series of CuCo_x catalysts with trace amounts of Co (0.07-1.8 at%) decorated on the surface of Cu nanowires using a simple dip coating method. Our



© The Author(s) 2024. **Open Access** This article is licensed under a Creative Commons Attribution 4.0 International License (<https://creativecommons.org/licenses/by/4.0/>), which permits unrestricted use, sharing, adaptation, distribution and reproduction in any medium or format, for any purpose, even commercially, as long as you give appropriate credit to the original author(s) and the source, provide a link to the Creative Commons license, and indicate if changes were made.



results revealed a volcano-shaped correlation between Co loading and C_{2+} selectivity, with the $CuCo_{0.4\%}$ catalyst exhibiting a 2-fold increase in C_{2+} selectivity compared to the Cu nanowire sample. *In situ* Raman and Infrared spectroscopies suggested that an optimal amount of Co could stabilize the Cu oxide/hydroxide species under the CO_2RR condition and promote the adsorption of CO, thus enhancing the C_{2+} selectivity. This work expands the potential for developing Cu-based bimetallic catalysts for CO_2RR .

Keywords: Electrochemical CO_2 reduction, copper cobalt catalyst, multi-carbon products, reaction mechanism, *in situ* techniques

INTRODUCTION

Electrochemical reduction of CO_2 (CO_2RR) under ambient conditions is a promising approach to mitigate the increasing concentration of CO_2 in the atmosphere and produce high value-added products.^[1] Cu-based materials have been extensively studied as catalysts for CO_2RR , as Cu is reported to be the only metal that can reduce CO_2 to various multi-carbon (C_{2+}) products, including gaseous hydrocarbons (e.g., C_2H_4 and C_2H_6) and liquid oxygenates (e.g., ethanol and propanol).^[2-9] However, the selectivity of C_{2+} on pure Cu is poor because the competing reactions, such as hydrogen evolution (HER) and CO_2 -to- C_1 (e.g., CO and HCOOH) reactions, require similar (or even lower) overpotentials compared to those for CO_2 -to- C_{2+} reactions.

To date, various strategies have been applied to improve the selectivity of C_{2+} over Cu-based catalysts, including tuning the exposed facets^[10], adjusting the oxidation state^[11], introducing defects^[12], and engineering the electrode structure^[13] and hydrophobicity^[14]. Among them, introducing a second metal to Cu has attracted great attention^[6,15]. For instance, recent studies of Cu-Au,^[16] Cu-Ag,^[7] and Cu-Zn^[17] catalysts have shown enhanced selectivity towards C_{2+} products. Notably, in these cases, the second metals (i.e., Au, Ag and Zn) are intrinsically selective for electrochemically reducing CO_2 to CO due to their weak binding strength with CO. Therefore, these metals can serve as a CO reservoir to enhance the $\ast CO$ coverage on Cu surface, thus increasing the C-C coupling probability^[1]. In contrast, many other metals, such as Fe, Ni, Co, *etc.*, are intrinsically not selective for CO_2RR because CO can strongly adsorb on these metals, leading to the poisoning of the catalyst surface and the high H_2 selectivity. Thus, most researchers have tried to remove these metals during the sample and electrolyte preparation^[18]. Interestingly, recent attempts have shown that Ni-Cu and Co-Cu alloys can also be active for CO_2RR . However, the selectivity of these catalysts varies for products such as CO, HCOOH, and C_2H_4 , and the enhanced catalytic activity is believed to result from adjustments in the d-band structure, size effects, and/or additional binding sites^[19-21]. Thus, further investigations are necessary to improve the design of such bimetallic catalysts. Building upon prior findings, we hypothesize that by strategically incorporating Group VIII metals (e.g., Co) onto the Cu surface and precisely adjusting their atomic ratios, it is possible to optimize the surface state of Cu and enhance the adsorption strength of $\ast CO$, ultimately improving selectivity for C_{2+} products.

Therefore, this work successfully designed and synthesized Cu nanowires (NWs) decorated with trace amounts of Co ($CuCo_x$, $x = 0.07\%$, 0.4% , and 1.8%) as advanced electrocatalysts for CO_2RR . A simple dip coating method developed in our previous studies was applied to ensure that Co was deposited on the surface of Cu and avoid contamination by surfactants^[22]. We found that with an optimal loading of Co (i.e., $CuCo_{0.4\%}$), the C_{2+} selectivity was doubled than that of pure Cu, reaching $> 40\%$ faradaic efficiency (FE) at $-1.0 V$ vs. reversible hydrogen electrode (RHE). *In situ* Raman and attenuated total reflectance-surface-enhanced infrared absorption spectroscopy (ATR-SEIRAS) revealed that the mixed Cu oxide states stabilized by Co could enhance the adsorption of $\ast CO$ intermediates and consequently promote the C_{2+} selectivity.

EXPERIMENTAL

CuCo_x ($x = 0.07\%$, 0.4% , and 1.8%) catalysts were prepared using a simple dip coating method (Experimental details in [Supplementary Materials](#)). Briefly, a piece of Cu foil was first immersed in a mixed solution of NaOH and (NH₄)₂S₂O₄ for 10 min to chemically oxidize its surface layers to grow Cu(OH)₂ NWs. This sample is named Cu NWs in the remainder of the paper to simplify the notation. The CuCo_x samples were produced via immersing these Cu NWs in aqueous Co(NO₃)₂ solution for 30 s to adsorb cobalt species, followed by heat treatment at 150 °C and electrochemical reduction under CO₂RR condition (i.e., -0.8 V vs. RHE in 0.1 M KHCO₃ for 20 min) [[Figure 1A](#)]^[22]. The atomic ratio of Co:Cu of the CuCo_x samples was tuned by changing the concentration of the Co(NO₃)₂ solution from 2 to 50 mM.

RESULTS AND DISCUSSION

The morphology of the Cu NWs and CuCo_x samples was studied using a scanning electron microscope (SEM) [[Supplementary Figure 1](#)]. Well-defined NW structure with an average length of ~10 μm and width of ~200 nm is observed [[Figure 1B](#)]. Notably, the NW morphology of the Cu sample did not change after Co deposition. This can be ascribed to the low concentration of the Co(NO₃)₂ solution and the short dipping time [[Supplementary Figure 1](#)]. The X-ray diffraction patterns (XRD) of CuCo_x samples were the same as those of the Cu NWs sample, with high-intensity diffraction peaks from metallic Cu [[Figure 1C](#)]. This indicates metallic Cu dominates the composition in the Cu NWs and CuCo_x samples. Characteristic diffraction peaks of Co-related crystal phases were not observed. This can be attributed to the low loading of Co as well.

We further examined the surface compositions of the Cu NWs and CuCo_x samples using X-ray photoelectron spectroscopy (XPS) analysis after each sample preparation step. In the case of the Cu NW sample, Cu stayed in Cu(OH)₂ form (not shown). As shown in [Figure 1D](#), Cu remained as Cu(OH)₂ with Cu 2p peaks at 934.7 and 954.6 eV after Co deposition. It turned to the form of CuO after the heat treatment due to dehydration. After pre-electrochemical reduction treatment, the Cu 2p peak shifted to a lower binding energy and the satellite peaks disappeared, indicating that CuO was reduced to Cu⁰/Cu¹⁺ species^[23,24]. Importantly, Co 2p peaks were found in the XPS, although with low intensities [[Supplementary Figure 2](#)], demonstrating the successful decoration of Co on Cu NWs.

To gain detailed information of the microstructure and the elemental distribution, high-angle annular dark-field scanning transmission electron microscopy (HAADF-STEM) and energy dispersive X-ray spectroscopy (EDX) measurements were performed. As shown in [Figure 1E](#), the STEM-coupled EDX mapping further corroborates the successful deposition of Co on Cu NWs. Notably, Co species are highly dispersed, as observed from the high-resolution transmission electron microscopy (TEM) images and the EDX mapping. Selected area electron diffraction (SAED) analysis was then conducted to investigate the crystal structure of the NWs [[Supplementary Figure 3](#)]. Only metallic Cu diffraction rings were observed. This proved that the NWs are metallic Cu-dominated, although the surfaces were oxidized. The SAED analysis and the XRD results demonstrate that the Cu species mainly consists of crystalline Cu both in the NWs and the Cu foils of the Cu NWs and CuCo_x samples. In addition, all studied samples showed the same diffraction ring, suggesting that the bulk crystal structure did not change noticeably from the Cu NWs to CuCo_x samples with varying amounts of Co deposited. No Co diffractions were observed in SAED, consistent with the XRD results, further implying that no long-range ordered cobalt species were present. This can be due to the low loading and high dispersion of Co.

Next, we performed electrochemical OH adsorption to study the influence of Co on the surface structure of the CuCo_x samples. In cyclic voltammograms (CVs), OH adsorption peaks exhibited distinctly at various

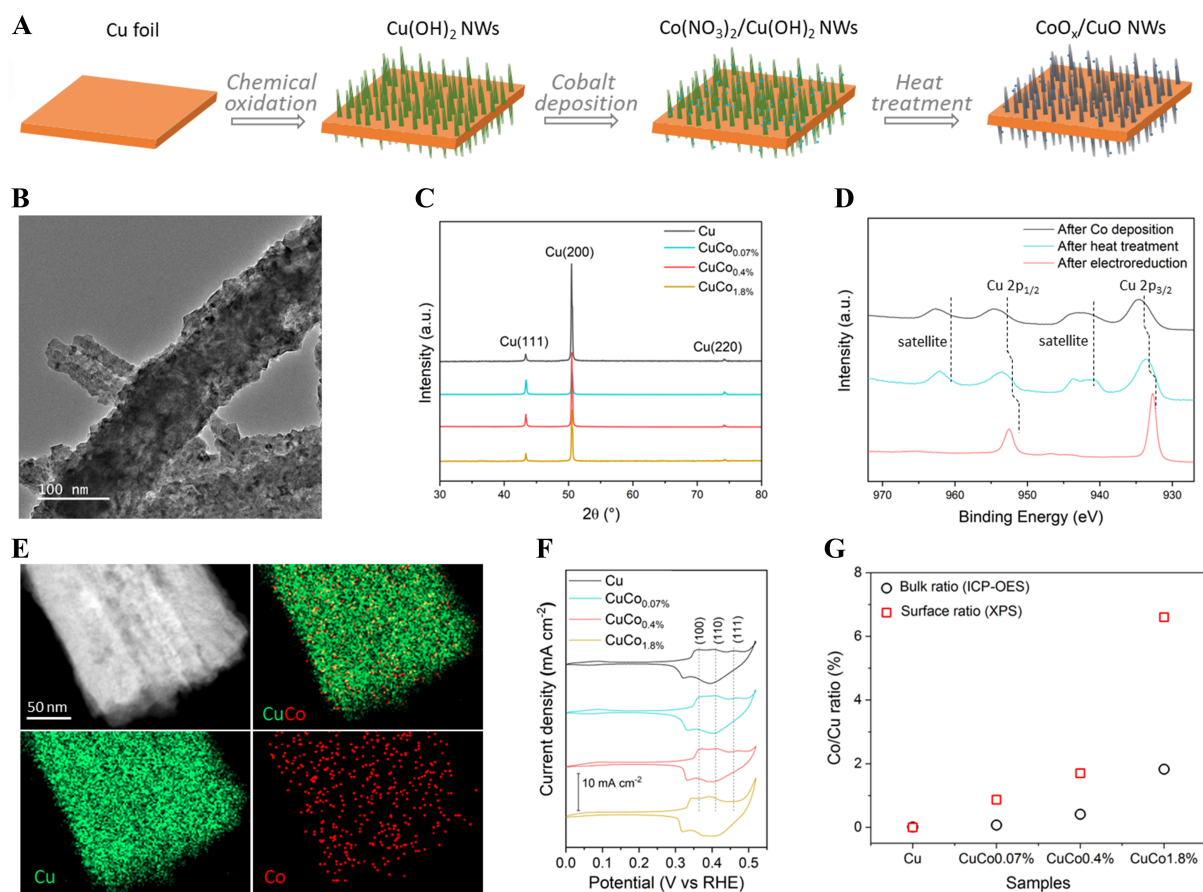


Figure 1. (A) Schematic illustration for synthesizing CoO_x/CuO NWs; samples after electroreduction during CO_2RR are denoted as CuCo_x catalysts; (B) Representative TEM image of the $\text{CuCo}_{0.4\%}$ sample; (C) XRD of Cu and CuCo_x catalysts; (D) Cu 2p XPS spectra of $\text{CuCo}_{0.4\%}$ after Co deposition, heat treatment, and electroreduction; (E) Element maps the $\text{CuCo}_{0.4\%}$ sample; (F) Cyclic voltammograms recorded in N_2 purged 1.0 M KOH capturing the surface-specific adsorption of oxygen (OH); (G) Bulk and surface atomic ratios of Co:Cu for Cu and CuCo_x catalysts obtained using ICP-OES and XPS, respectively. NWs: Nanowires; CO_2RR : CO_2 reduction reaction; TEM: transmission electron microscopy; XRD: X-ray diffraction patterns; XPS: X-ray photoelectron spectroscopy; ICP-OES: inductively coupled plasma optical emission spectrometry.

potentials on distinct facets of Cu crystals, thus allowing the probing of surface structure of Cu^[25,26]. As shown in Figure 1F, three OH desorption peaks assigned to Cu (111), (110), and (100) facets were observed for the Cu NWs and CuCo_x samples. These peaks are almost identical for the Cu, $\text{CuCo}_{0.07\%}$, and $\text{CuCo}_{0.4\%}$ samples. However, the peak positions were shifted to ~ 0.02 V lower for the $\text{CuCo}_{1.8\%}$ sample, indicating a weaker binding of OH on this sample surface. Intriguingly, the (111) peak for $\text{CuCo}_{1.8\%}$ almost diminished, indicating that the surface structure of Cu was only affected by a high loading of Co. To conclude, using a simple dip coating method, a series of CuCo_x catalysts with highly dispersed Co decorated on the surface of Cu NWs were successfully synthesized. In addition, the Co:Cu ratio in the catalyst was quantitatively analyzed by XPS and inductively coupled plasma optical emission spectrometry (ICP-OES). Quantitative determination of the surface Co:Cu ratio from the XPS analysis showed a fast increase from $\text{CuCo}_{0.07\%}$ to $\text{CuCo}_{1.8\%}$. Interestingly, when compared with the bulk Co:Cu ratio measured with the ICP-OES, the Co concentration on the surface is much higher than that in the bulk of the CuCo_x samples [Figure 1G]. This is similar to our previous findings, which show that the dip coating method allows the deposition of metal species to concentrate on the surface of the NWs^[22].

The CO₂RR activity and product distribution from Cu NWs and CuCo_x samples were evaluated in CO₂-saturated 0.1 M KHCO₃ electrolyte within a two-compartment H-cell. The geometric current densities in the potential range of -0.6 to -1.2 V vs. RHE are shown in Figure 2. Cu and CuCo_x catalysts show very similar geometric current densities in the entire potential range [Figure 2A]. This could be attributed to their similar morphology and almost identical electrochemical active surface area (ECSA) [Supplementary Figure 4], as SEM results showed that the Cu NW structure was well preserved after Co deposition [Supplementary Figure 1].

To assess the influence of Co on the catalytic selectivity, gas and liquid products were analyzed using gas chromatography (GC) and ¹H nuclear magnetic resonance (NMR), respectively. The FEs of the reaction products are presented in Figure 2B and C and Supplementary Figure 4. Since Co is known to be more active than Cu towards HER, high loading of Co (i.e., CuCo_{1.8%} with 6.6 at% coverage of surface Co, as shown in Figure 1G) enhances HER performance unsurprisingly compared to Cu NWs. However, CuCo_{0.07%} and CuCo_{0.4%} show similar H₂ selectivity in the low overpotential range (-0.6 to -0.9 V vs. RHE) and 10%-20% lower H₂ selectivity at higher overpotentials (-1.0 to -1.2 V vs. RHE) [Supplementary Figure 5] compared to Cu NWs. The reduction products of CO₂ were influenced more dramatically due to the decoration of Co. As shown in Figure 2B and C, the CO FEs of all three CuCo_x samples were significantly lower than those of the Cu NWs, and C₂₊ FEs of these CuCo_x samples were significantly higher than those of the Cu NWs. Specifically, the highest FE for C₂₊ increased sharply from 19.5% for Cu to 33.2% for CuCo_{0.07%}, 40.7% for CuCo_{0.4%}, and 26.0% for CuCo_{1.8%}. CO is widely accepted as the key reaction intermediate for converting CO₂ to C₂₊ on Cu. The fast decrease of CO detected by GC in Figure 2B can be ascribed to the accelerated consumption of the adsorbed *CO on the surface in forming C₂₊, resulting in decreased desorbed CO. The above results suggest that Co plays an important role in lowering gaseous CO release and facilitating C₂₊ production. Meanwhile, the suppressed H₂ production on CuCo_x samples compared to Cu NWs could also contribute to the more effective C₂₊ production, as more electrons were consumed by C-C coupling instead of HER.

Intriguingly, the selectivity of C₂₊ products increases with Co loading until 0.4 at%, but then decreases with further Co loading (1.8 at%) [Figure 2C]. To verify this trend, we prepared two additional Co-modified Cu catalysts with 0.2% (CuCo_{0.2%}) and 1.1% Co (CuCo_{1.1%}) and tested their CO₂RR performance under identical conditions. As shown in Figure 2D, the FEs for C₂H₄ and C₂H₅OH of the Cu and CuCo_x samples obtained at -1.0 V vs. RHE demonstrate a volcano-shape dependence on the Co loading, where the CuCo_{0.4%} catalyst displays the highest FE for both C₂H₄ (27.3%) and C₂H₅OH (10.7%) productions. This performance surpasses that of the state-of-the-art CuCo catalysts currently reported in the literature [Supplementary Table 1]. As the morphology and the ECSA of the Cu NWs and CuCO_x samples are very similar, the influence of the local reaction environment can thus be ruled out. Therefore, these results demonstrate that an optimal loading of Co could effectively improve the selectivity of Cu towards C₂₊ products by suppressing the H₂ evolution and accelerating C-C coupling, which is consistent with previous research^[21,27].

To understand the enhanced selectivity towards C₂₊ products on CuCo_x catalysts, *in situ* surface-enhanced Raman spectroscopy (SERS) was employed to probe the adsorbed intermediates on the catalyst surfaces^[2,28]. The NW structure of the Cu and CuCo_x catalysts was reported to enhance Raman signals; thus, additional surface manipulation was not required^[29,30]. We first examined the surface of CuCo_{0.4%} as it showed the highest performance of C₂₊ production. Figure 3A shows the potential-dependent SERS spectra of CuCo_{0.4%} acquired in CO₂-saturated 0.1 M KHCO₃ electrolyte at different applied potentials. At open circuit potential (OCP), the CuCo_{0.4%} samples exhibited three characteristic Raman bands of CuO at around ~300, ~350, and ~590 cm⁻¹^[31]. These peaks disappeared after applying a reduction potential of -0.4 V vs. RHE, demonstrating

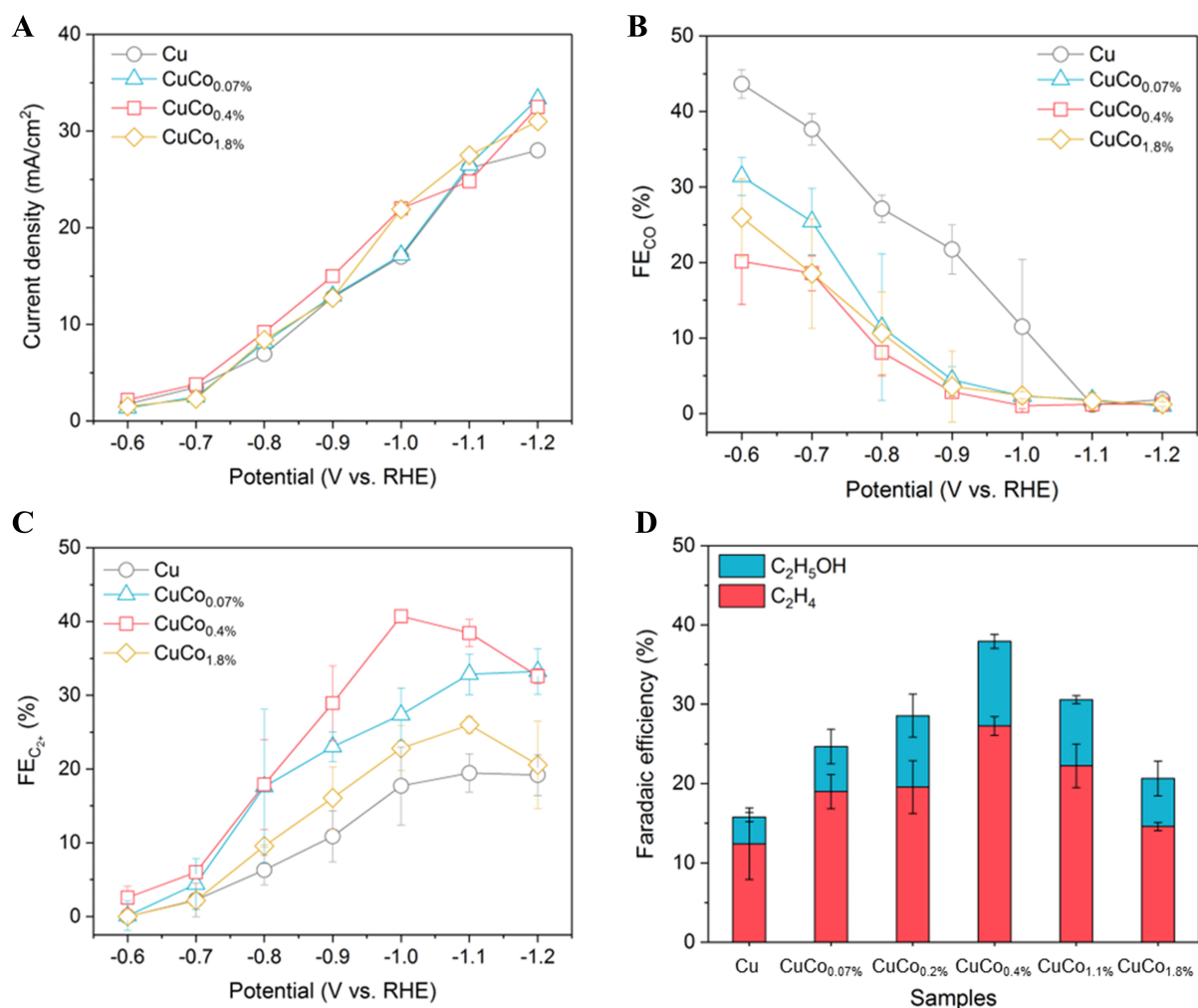


Figure 2. (A) Current density, (B) Faradaic efficiency of CO, and (C) Faradaic efficiency of C₂₊ for Cu, CuCo_{0.07%}, CuCo_{0.4%} and CuCo_{1.8%}; (D) Faradaic efficiency of C₂H₄ and C₂H₅OH for CuCo samples with different amounts of Co. Error bars are means \pm SD ($n = 3$ replicates). C₂₊: Multi-carbon.

that the CuO in bulk can be reduced promptly at potentials more negative than -0.4 V vs. RHE, which agrees with our XRD and SAED analysis. However, two weak bands at ~ 490 and ~ 570 cm⁻¹ attributable to the surface Cu oxide/hydroxide species [e.g., a mixture of CuO_x and Cu(OH)_y], named as CuO_x/(OH)_y, are present after reduction^[29,32,33]. These oxidized Cu species could be attributed to the dynamic oxidation of the Cu surface and the adsorption of -OH groups during the CO₂RR and HER processes^[29,32]. In addition, three Raman bands related to *CO can be observed in the potential range of -0.6 to -0.8 V vs. RHE: the two low-frequency bands at ~ 280 and ~ 360 cm⁻¹ can be assigned to the frustrated rotation and stretching vibration of Cu-CO, respectively; and the high-frequency broad band located between $1,950$ and $2,100$ cm⁻¹ is caused by intramolecular C \equiv O stretching vibrations with various binding configurations^[30,34]. Both the surface Cu oxide species and the *CO-related intermediates disappeared after removing the applied potential, indicating that these species are generated and stabilized under the CO₂RR condition^[35].

To explore the influence of Co deposition on the CO₂RR process, SERS was also employed to probe the surface speciation of Cu, CuCo_{0.07%}, and CuCo_{1.8%} samples. As shown in Figure 3B, all four samples share similar spectral features at a reduction potential of -0.8 V, suggesting the presence of similar surface species.

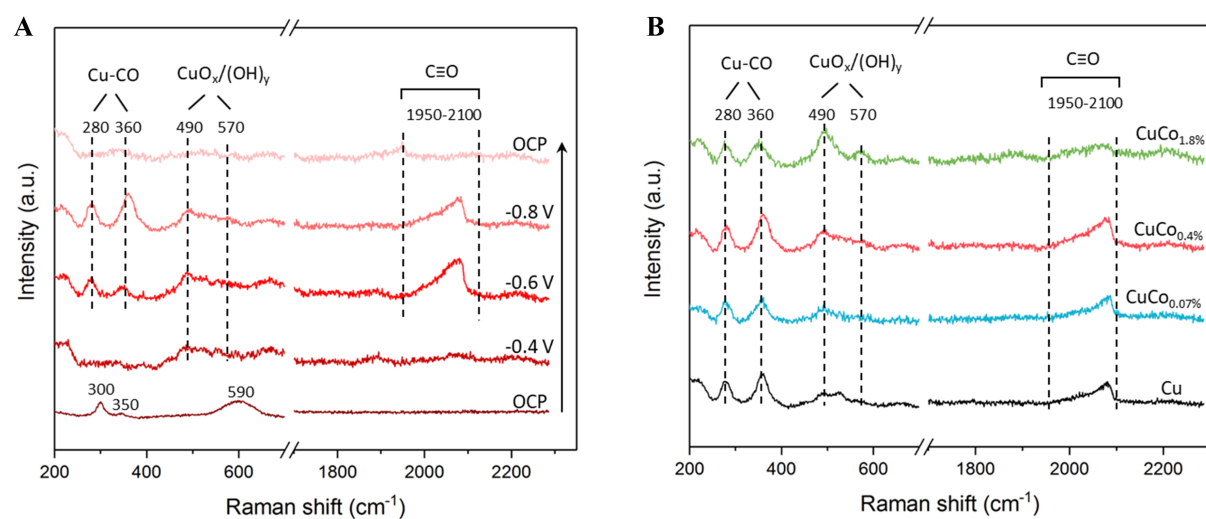


Figure 3. *In situ* Raman spectra of (A) $\text{CuCo}_{0.4\%}$ at different applied potentials; and (B) various CuCo_x samples at -0.8 V vs. RHE in CO_2 saturated 0.1 M KHCO_3 . RHE: Reversible hydrogen electrode.

However, the relative intensities of these peaks differ [Supplementary Figure 6]. While the peak intensity of $\text{CuO}_x/(\text{OH})_y$ increases with Co deposition amount, the Cu-CO and C≡O peak intensities are maximized for the $\text{CuCo}_{0.4\%}$ sample. The trend for $\text{CuO}_x/(\text{OH})_y$ peak intensity agrees with previous studies that showed that isolated Co atoms could stabilize the Cu_2O surface by increasing the activation barrier of surface oxygen abstraction^[36]. The trend for Cu-CO and C≡O peak intensities are in line with the C_{2+} selectivity observed in Figure 2C, indicating that high CO coverage is the obvious reason for C–C coupling, therein, a higher C_{2+} production^[7,13]. Various studies have shown that mixed oxide states of Cu could enhance the CO_2 -to- C_{2+} conversion^[11,37–39]. For instance, by using density functional theory (DFT) calculations and *in situ* SEIRAS, Zhang *et al.* demonstrated that the $\text{Cu}^{\delta+}$ site at the $\text{Cu}^0/\text{Cu}^{\delta+}$ interface favors the formation of CHO intermediates, which can subsequently couple with CO on adjacent Cu^0 surfaces to form OCCHO intermediates, promoting the generation of C_{2+} products^[40]. In our case, we anticipate that the $\text{CuCo}_{0.4\%}$ sample shows higher C_{2+} selectivity than the other samples due to the coexistence of Cu^0 and $\text{Cu}^{\delta+}$ species in an optimized ratio.

Notably, due to the low loading of Co, we could not detect any vibrational bands associated with Co species or reaction intermediates adsorbed on Co. However, the role of Co species in tuning the reaction pathway should not be ignored since the binding of CO and H to the Co surface is much stronger than that to the Cu surface, which can certainly affect the reaction pathways^[41,42]. Further, a recent study shows that in CuCo single atom alloys, Cu sites neighboring Co atomic sites could accelerate CO_2 -to- CO conversion and Cu-Co sites also favor the deoxygenation of HOCCH , which increases the selectivity toward ethylene over ethanol^[43]. More recently, Luo *et al.* found that Co in cobalt phthalocyanine could promote the C_2 selectivity of Cu catalysts because the adsorption of CO_2 , CO , and CO_2RR intermediates could be enhanced on both Co and Cu sites^[44]. These results indicate that using strong CO-binding elements to promote the C_{2+} selectivity of Cu is effective, and further mechanism understanding is also required.

To further investigate the formation mechanism of C_{2+} products on the CuCo_x catalysts, *in situ* ATR-SEIRAS was performed over the Cu and $\text{CuCo}_{0.4\%}$ catalysts. Figure 4A shows almost no characteristic peak of CO species detected on the surface of the Cu NWs electrode during the electrocatalytic process. However, on the $\text{CuCo}_{0.4\%}$ sample [Figure 4B], a peak appears at a wavelength of $2,080$ cm^{-1} from -0.4 V vs. RHE and

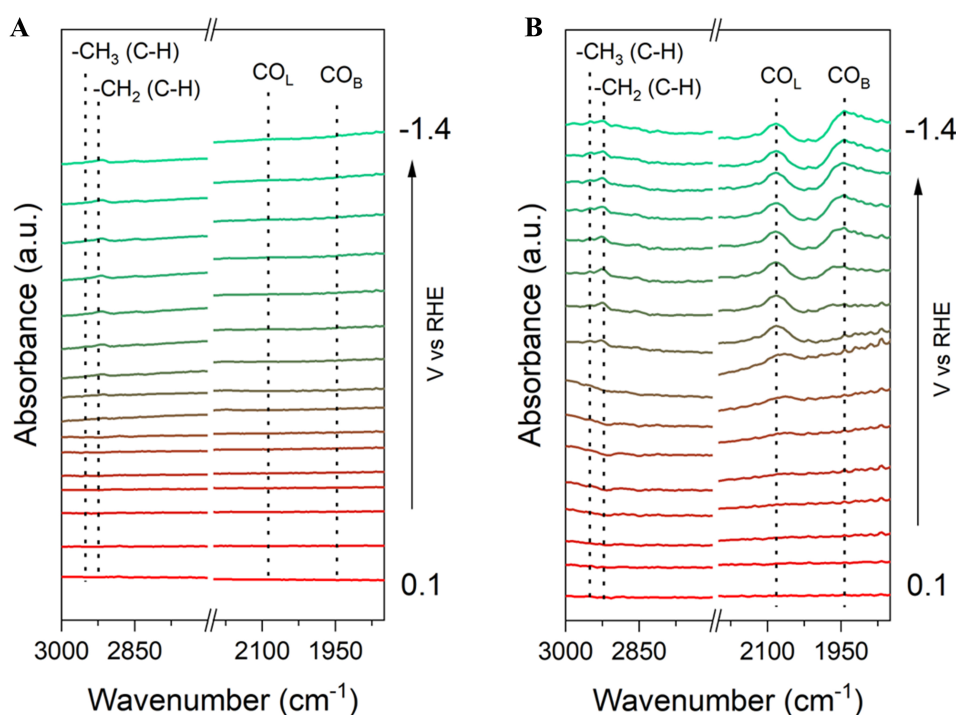


Figure 4. Potential-dependent ATR-SEIRAS spectra for (A) Cu and (B) CuCo_{0.4%} at 0.1 to -1.4 V vs. RHE in CO₂-saturated 0.1 M KHCO₃. The spectrum taken at 0.2 V vs. RHE was used as the reference. ATR-SEIRAS: Attenuated total reflectance-surface-enhanced infrared absorption spectroscopy; RHE: reversible hydrogen electrode.

another at 1,950 cm⁻¹ from -0.8 V vs. RHE. These peaks can be assigned to the adsorbed ^{*}CO species, with the first one belonging to linear adsorption (^{*}CO_L) and the second one to bridge adsorption (^{*}CO_B), respectively^[45]. Further, two additional peaks appear at 2,952 and 2,923 cm⁻¹ for both Cu NWs and CuCo_{0.4%} samples with relatively low intensities, attributed to the C-H extension of methyl (-CH₃) and methylene (-CH₂), respectively, in agreement with the observed CH₃CH₂OH production on these catalysts^[46]. Overall, the *in situ* ATR-SEIRAS results indicate a higher ^{*}CO coverage on the CuCo_{0.4%} surface than the Cu NWs surface, and the reason could be the higher ^{*}CO adsorption energy on CuCo surfaces than pure Cu surfaces. Consequently, the high ^{*}CO coverage could facilitate the formation of C₂₊ products on the CuCo_{0.4%} sample^[4]. Consistent with the *in situ* Raman results, the optimal adsorption of ^{*}CO species and subsequent C-C coupling can be attributed to the synergistic effect between Cu and Co metals and the coexistence of reduced and oxidized Cu species.

CONCLUSIONS

In summary, this work shows that Co, despite being a non-CO₂RR selective metal, can be used to decorate the Cu surface to improve the selectivity towards C₂₊ products. With an optimized amount of Co, the CuCo_{0.4%} sample showed 40.7% FE for C₂₊ at -1.0 V vs. RHE, two times higher than that of the Cu sample (19.5%). *Ex situ* techniques indicated that with a low deposition amount of Co, the crystal structure and morphology of Cu NWs were not influenced. However, *in situ* Raman spectra revealed that Co could stabilize the Cu^{δ+} species on the CuCo_x surface, and *in situ* infrared spectroscopy indirectly proves that coexistence of Co, Cu⁰ and Cu^{δ+} may promote the adsorption of ^{*}CO, thus accelerating the C-C coupling. We believe this study can inspire the development of other Cu-based bimetallic catalysts for CO₂RR.

DECLARATIONS

Authors' contributions

Conceptualized and supervised the project: Luo W, Zhao K, Züttel A
Synthesized the catalysts and performed the electrochemical tests: Soodi S
Performed the *in situ* analysis: Zhang JJ
Performed sample characterizations and data analysis: Zhang J, Liu Y, Luo W
Co-wrote the manuscript: Soodi S, Zhang JJ, Zhao K, Luo W
Reviewed the paper: Lashgari M, Zafeiratos S, Züttel A
All the authors discussed the results and revised the manuscript.

Availability of data and materials

The data that support the findings of this study are available from the corresponding author upon reasonable request.

Financial support and sponsorship

This research was supported by the Swiss National Science Foundation (Ambizione project PZ00P2_179989).

Conflicts of interest

Liu Y is the Guest Editor of the Special Issue “Carbon in Catalysis” and the Junior Editorial Board Member of the Journal of *Chemical Synthesis*, while the other authors have declared that they have no conflicts of interest.

Ethical approval and consent to participate

Not applicable.

Consent for publication

Not applicable.

Copyright

© The Author(s) 2024.

REFERENCES

1. De Luna P, Hahn C, Higgins D, Jaffer SA, Jaramillo TF, Sargent EH. What would it take for renewably powered electrosynthesis to displace petrochemical processes? *Science* 2019;364:eaav3506. DOI PubMed
2. Pham THM, Zhang J, Li M, et al. Enhanced electrocatalytic CO₂ reduction to C₂₊ products by adjusting the local reaction environment with polymer binders. *Adv Energy Mater* 2022;12:2103663. DOI
3. Zhang J, Luo W, Züttel A. Crossover of liquid products from electrochemical CO₂ reduction through gas diffusion electrode and anion exchange membrane. *J Catal* 2020;385:140-5. DOI
4. Zhang J, Luo W, Züttel A. Self-supported copper-based gas diffusion electrodes for CO₂ electrochemical reduction. *J Mater Chem A* 2019;7:26285-92. DOI
5. Koolen CD, Luo W, Züttel A. From single crystal to single atom catalysts: structural factors influencing the performance of metal catalysts for CO₂ electroreduction. *ACS Catal* 2023;13:948-73. DOI
6. Koolen CD, Oveisi E, Zhang J, et al. Low-temperature non-equilibrium synthesis of anisotropic multimetallic nanosurface alloys for electrochemical CO₂ reduction. *Nat Synth* 2024;3:47-57. DOI
7. Zhang J, Pham THM, Ko Y, et al. Tandem effect of Ag@C@Cu catalysts enhances ethanol selectivity for electrochemical CO₂ reduction in flow reactors. *Cell Rep Phys Sci* 2022;3:100949. DOI
8. Zhang J, My Pham TH, Gao Z, et al. Electrochemical CO₂ reduction over copper phthalocyanine derived catalysts with enhanced selectivity for multicarbon products. *ACS Catal* 2023;13:9326-35. DOI
9. Gao Y, Xiao H, Ma X, et al. Cooperative adsorption of interfacial Ga-N dual-site in GaOOH@N-doped carbon nanotubes for enhanced electrocatalytic reduction of carbon dioxide. *J Colloid Interface Sci* 2024;654:339-47. DOI PubMed
10. Zhong D, Zhao ZJ, Zhao Q, et al. Coupling of Cu(100) and (110) facets promotes carbon dioxide conversion to hydrocarbons and alcohols. *Angew Chem Int Ed Engl* 2021;60:4879-85. DOI PubMed

11. Yang PP, Zhang XL, Gao FY, et al. Protecting copper oxidation state via intermediate confinement for selective CO₂ electroreduction to C₂₊ fuels. *J Am Chem Soc* 2020;142:6400-8. DOI PubMed
12. Tang C, Shi J, Bai X, et al. CO₂ reduction on copper's twin boundary. *ACS Catal* 2020;10:2026-32. DOI
13. Zhang T, Bui JC, Li Z, Bell AT, Weber AZ, Wu J. Highly selective and productive reduction of carbon dioxide to multicarbon products via in situ CO management using segmented tandem electrodes. *Nat Catal* 2022;5:202-11. DOI
14. García de Arquer FP, Dinh CT, Ozden A, et al. CO₂ electrolysis to multicarbon products at activities greater than 1 A cm⁻². *Science* 2020;367:661-6. DOI PubMed
15. Zhou F, Zhang J, Zhang Y, Wu Y, Wang Y, Luo W. Palladium-copper bimetallic catalysts for electroreduction of CO₂ and nitrogenous species. *Coord Chem Rev* 2024;509:215802. DOI
16. Morales-guio CG, Cave ER, Nitopi SA, et al. Improved CO₂ reduction activity towards C₂₊ alcohols on a tandem gold on copper electrocatalyst. *Nat Catal* 2018;1:764-71. DOI
17. Ren D, Gao J, Pan L, et al. Atomic layer deposition of ZnO on CuO enables selective and efficient electroreduction of carbon dioxide to liquid fuels. *Angew Chem* 2019;131:15178-82. DOI
18. Hori Y, Murata A, Takahashi R. Formation of hydrocarbons in the electrochemical reduction of carbon dioxide at a copper electrode in aqueous solution. *J Chem Soc Faraday Trans 1* 1989;85:2309-26. DOI
19. Xu C, Vasileff A, Jin B, et al. Graphene-encapsulated nickel-copper bimetallic nanoparticle catalysts for electrochemical reduction of CO₂ to CO. *Chem Commun* 2020;56:11275-8. DOI PubMed
20. Yan Y, Zhao Z, Zhao J, Tang W, Huang W, Lee J. Atomic-thin hexagonal CuCo nanocrystals with d-band tuning for CO₂ reduction. *J Mater Chem A* 2021;9:7496-502. DOI
21. Bernal M, Bagger A, Scholten F, et al. CO₂ electroreduction on copper-cobalt nanoparticles: size and composition effect. *Nano Energy* 2018;53:27-36. DOI
22. Luo W, Xie W, Mutschler R, et al. Selective and stable electroreduction of CO₂ to CO at the copper/indium interface. *ACS Catal* 2018;8:6571-81. DOI
23. Li M, My Pham TH, Ko Y, et al. Support-dependent Cu–In bimetallic catalysts for tailoring the activity of reverse water gas shift reaction. *ACS Sustain Chem Eng* 2022;10:1524-35. DOI
24. Li M, Luo W, Züttel A. Near ambient-pressure X-ray photoelectron spectroscopy study of CO₂ activation and hydrogenation on indium/copper surface. *J Catal* 2021;395:315-24. DOI
25. Raciti D, Cao L, Livi KJT, et al. Low-overpotential electroreduction of carbon monoxide using copper nanowires. *ACS Catal* 2017;7:4467-72. DOI
26. Wang Y, Raciti D, Wang C. High-flux CO reduction enabled by three-dimensional nanostructured copper electrodes. *ACS Catal* 2018;8:5657-63. DOI
27. Grote J, Zeradjanin AR, Cherevko S, et al. Screening of material libraries for electrochemical CO₂ reduction catalysts - Improving selectivity of Cu by mixing with Co. *J Catal* 2016;343:248-56. DOI
28. Luo W, Zhang Q, Zhang J, Moiola E, Zhao K, Züttel A. Electrochemical reconstruction of ZnO for selective reduction of CO₂ to CO. *Appl Catal B Environ* 2020;273:119060. DOI
29. Zhao Y, Chang X, Malkani AS, et al. Speciation of Cu surfaces during the electrochemical CO reduction reaction. *J Am Chem Soc* 2020;142:9735-43. DOI PubMed
30. Jiang S, Klingan K, Pasquini C, Dau H. New aspects of operando Raman spectroscopy applied to electrochemical CO₂ reduction on Cu foams. *J Chem Phys* 2019;150:041718. DOI PubMed
31. Deng Y, Handoko AD, Du Y, Xi S, Yeo BS. In Situ Raman spectroscopy of copper and copper oxide surfaces during electrochemical oxygen evolution reaction: identification of Cu^{III} oxides as catalytically active species. *ACS Catal* 2016;6:2473-81. DOI
32. Moradzaman M, Mul G. In Situ Raman study of potential-dependent surface adsorbed carbonate, CO, OH, and C species on Cu electrodes during electrochemical reduction of CO₂. *ChemElectroChem* 2021;8:1478-85. DOI
33. Liu C, Gong J, Li J, et al. Preanodized Cu surface for selective CO₂ electroreduction to C₁ or C₂₊ products. *ACS Appl Mater Interfaces* 2022;14:20953-61. DOI PubMed
34. Li YC, Wang Z, Yuan T, et al. Binding site diversity promotes CO₂ electroreduction to ethanol. *J Am Chem Soc* 2019;141:8584-91. DOI PubMed
35. Lei Q, Huang L, Yin J, et al. Structural evolution and strain generation of derived-Cu catalysts during CO₂ electroreduction. *Nat Commun* 2022;13:4857. DOI PubMed PMC
36. Wang C, Kong Y, Soldemo M, et al. Stabilization of Cu₂O through site-selective formation of a Co₁Cu hybrid single-atom catalyst. *Chem Mater* 2022;34:2313-20. DOI
37. Chou TC, Chang CC, Yu HL, et al. Controlling the oxidation state of the Cu electrode and reaction intermediates for electrochemical CO₂ reduction to ethylene. *J Am Chem Soc* 2020;142:2857-67. DOI PubMed
38. Lee SY, Jung H, Kim NK, Oh HS, Min BK, Hwang YJ. Mixed copper states in anodized Cu electrocatalyst for stable and selective ethylene production from CO₂ reduction. *J Am Chem Soc* 2018;140:8681-9. DOI PubMed
39. Lei Q, Zhu H, Song K, et al. Investigating the origin of enhanced C₂₊ selectivity in oxide/hydroxide-derived copper electrodes during CO₂ electroreduction. *J Am Chem Soc* 2020;142:4213-22. DOI PubMed
40. Zhang XY, Lou ZX, Chen J, et al. Direct OC-CHO coupling towards highly C₂₊ products selective electroreduction over stable Cu⁰/Cu²⁺ interface. *Nat Commun* 2023;14:7681. DOI PubMed PMC

41. Li J, Xu A, Li F, et al. Enhanced multi-carbon alcohol electroproduction from CO via modulated hydrogen adsorption. *Nat Commun* 2020;11:3685. DOI PubMed PMC
42. Li J, Wang Z, McCallum C, et al. Constraining CO coverage on copper promotes high-efficiency ethylene electroproduction. *Nat Catal* 2019;2:1124-31. DOI
43. Kim B, Tan YC, Ryu Y, et al. Trace-level cobalt dopants enhance CO₂ electroreduction and ethylene formation on copper. *ACS Energy Lett* 2023;8:3356-64. DOI
44. Luo Y, Yang J, Qin J, et al. Cobalt phthalocyanine promoted copper catalysts toward enhanced electro reduction of CO₂ to C₂: synergistic catalysis or tandem catalysis? *J Energy Chem* 2024;92:499-507. DOI
45. Jiang T, Qin X, Ye K, et al. An interactive study of catalyst and mechanism for electrochemical CO₂ reduction to formate on Pd surfaces. *Appl Catal B Environ* 2023;334:122815. DOI
46. Yan W, Li G, Cui S, et al. Ga-modification near-surface composition of Pt-Ga/C catalyst facilitates high-efficiency electrochemical ethanol oxidation through a C2 intermediate. *J Am Chem Soc* 2023;145:17220-31. DOI PubMed